

# Aggregating lane markings into lanes for intersection assistance

Christian Duchow and Björn Körtner

**Abstract**—Driver assistance functions on marked innercity intersections require a reliable detection of intersection lanes. Due to the high complexity of intersection scenarios and the large amount of clutter that is usually encountered in urban areas, existing highway lane detectors are not applicable for this task. In order to detect the lanes on marked innercity intersections, we adopt a two step process of first detecting individual lane marking segments and then aggregating these segments to appropriate lanes. We assume that a lane detector for innercity scenarios should be capable of handling lanes with arbitrary orientation and curvature and thus may not rely on simple geometric models. In order to achieve this, in the paper we first derive a set of features from the lane marking segment data. These features are fed into a support vector machine. The support vector machine determines whether the lane marking segments belong to the same lane or not.

## I. INTRODUCTION

Driver assistance functions on marked intersections may increase traffic safety by guiding drivers through complex intersections and by issuing warnings of potential hazards. However, while the detection of lanes on highways as in [1], [2], [3] has already been brought to market, the detection of lanes on marked intersections is still an area of active research and one that will possibly play a key role in the DARPA Urban Challenge 2007. The fact that so far there is no flexible, general solution to the detection of lanes on marked intersections may be due to the complexity of intersections with arbitrary lane orientations, high lane curvature and overlapping lanes.

Although research on intersection recognition is still in an early stage, some relevant work has already been presented in the literature: [4] detects lanes on innercity intersections through the use of prior knowledge. A digital map is used to obtain structural information about topology and geometry of the whole intersection. Expert knowledge is then used to refine the information and arrive at a set of intersection hypotheses which are then compared to the image. [5] proposes an approach which also uses a digital map and derives intersection geometry hypotheses, though the approach is not as flexible and powerful as [4]. [6] proposes an approach to detect the presence of intersections and the lanes connected to them. The intersections themselves are not marked, thus, [6] does not strictly focus on detecting lanes on marked intersections.

Since digital maps may be out of date or not available, there is the need for researching detecting lanes on marked intersections without the use of digital map information.

C. Duchow is with the Institute of Measurement and Control Theory, University of Karlsruhe, Karlsruhe, Germany [duchow@mrt.uka.de](mailto:duchow@mrt.uka.de)

B. Körtner has completed the Masters of Computer Science at the University of Karlsruhe, Karlsruhe, Germany

Without any prior information about the present scene, we therefore lack the possibility to generate geometry hypotheses as in [4].

[7] is a work similar in spirit to ours. What [7] and our work have in common is that single lane marking segments are detected and then aggregated into lane boundaries. A key difference is that Enkelmann et al. employ a geometrical model for the lane boundaries while we do not. Lane geometry on intersections may be designed to fit innercity constraints like buildings and infrastructure rather than a typical shape, therefore we aim to achieve a higher applicability by refraining from using a geometrical model. In addition, an extension to support vector machines is capable of determining a measure of probability with which the classification is correct [8]. Furthermore, in our work we test for parallel lane boundaries in order to construct complete lanes rather than deliver lane boundaries.

We approach the task of detecting lanes on marked intersections in a two step procedure. The first step consists of detecting individual lane marking segments on the intersection. This may be accomplished with the use of the Canny [9] edge detector or other approaches [7] and will not be discussed in this paper. We have used the lane marking segment detector described in [10]. The second step is the focus of this paper and consists of detecting lanes in the set of detected lane marking segments. The single lane marking segment hypotheses are described with the properties width  $W$ , length  $L$ , orientation  $\alpha$  and position  $\mathbf{X} = [Y, Z]^T$ . In addition to these geometrical properties, there are three measures which describe the quality of a lane marking segment hypotheses.  $\Delta g = g_o - g_i$  is the difference between the average grey value inside the lane marking segment  $g_i$  and the area outside the lane marking segment  $g_o$ .  $\sigma_i$  is the standard deviation of the grey value inside the lane marking segment and  $\sigma_o$  is the standard deviation of the grey value outside the lane marking segment. These values are provided by the lane marking segment detector. For a good lane marking segment, we expect a high  $\Delta g$  and small  $\sigma_i$  and small  $\sigma_o$ . An illustration of an example set of single lane marking segment hypotheses lying in the ground plane  $X = 0$  is given in Fig. 1. Our task is to determine which of these lane marking segments belong to the same lane and which lane marking segment hypotheses are clutter. The desired aggregation result for the data visualized in Fig. 1 is shown in Fig. 2. The lane has been detected while the clutter has been ignored. Due to space constraints, this example does not show the more interesting case where there are at least two curved, overlapping lanes in the scene. Even in this simple case, the detection of the correct left lane boundary requires picking only the four

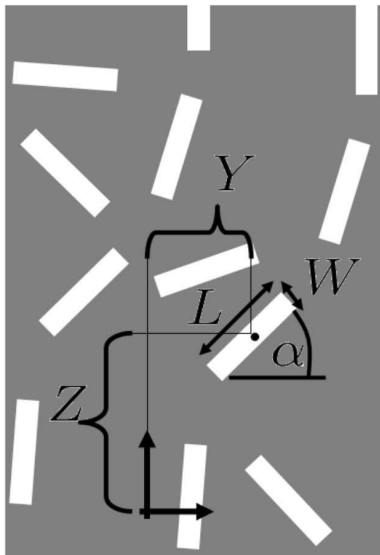


Fig. 1. An example set of single lane marking segment hypotheses.

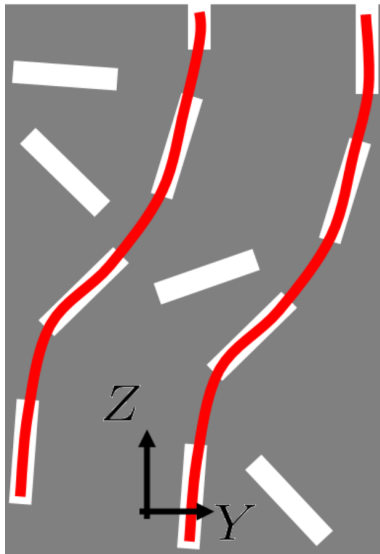


Fig. 2. The aggregation result recognizes the lane while rejecting the clutter.

correct lane markings while suppressing eight other lane marking segments.

Section II first describes the formation of triplets of individual lane marking segments. A lane marking segment may belong to several triplets. We then compute features describing the triplets. The features are then fed into a support vector machine which determines whether the lane marking segments in the triplet belong to the same lane boundary or not. Section II gives a detailed description of the features that we use for the classification. We then describe how the triplets are combined into lane boundaries. Section III shows results obtained with real imagery.

## II. DETECTION OF LANES

### A. Preprocessing

A detection of lanes on innercity intersections must be capable of handling curved lanes and should not be restricted to any particular geometrical form. Thus, the important question arises how to determine whether some lane marking segments form a lane without matching the segments to a geometrical model. Another, related issue is how to select exactly the correct lane marking segments and successfully ignore all the others while detecting each single lane boundary. Clearly, when considering a single lane boundary on an intersection, the lane marking segments belonging to other lane boundaries must be treated as outliers. Consequently, an approach to solve this issue must be focused on the local neighborhood of the lane marking segments in question.

In our approach, this local neighborhood is established by forming triplets of single lane marking segments. The segments in a triplet are always positioned close to each other and are evaluated according to the features described in the following subsections. The evaluation determines whether the segments in the triplet may belong to the same lane. This preprocessing is very optimistic about the lane membership, i.e., the thresholds in feature space are set such that we retain all correct triplets of lane marking segments. On the other hand, we also obtain a lot of false positive triplets of lane marking segments, though this number is still considerably lower than the number of all possible triplets in the set. For example, for a test set consisting of 908 correct triplets of lane marking segments detected in 295 video images, this preprocessing step finds 891 correct triplets and misses 17 correct triplets. It also produces 1789 wrong triplets. These results are satisfactory for the subsequent classification and lane detection steps. The decision whether a candidate triplet is accepted or rejected at this stage is based upon simple thresholds in each feature dimension. We have chosen to form triplets because with three segments we are able to derive information about the lane curvature. To consider more than three segments, i.e. form quadruples could be asking too much because in some images there may only be three segments available.

### B. Classification

This subsection describes the feature space which we use to evaluate the triplets that were formed and not rejected during preprocessing. The triplets serve as an intermediate stage between single lane marking segments and the final lane boundary. The triplet features are fed into a support vector machine which determines whether the individual lane markings in that triplet belong to the same lane boundary or not. This classification is more sophisticated than the preprocessing described in subsection II-A and eliminates most false positives.

We have found twelve feature types that have proven to be meaningful in determining lane boundary membership. In the following, a description of each of these feature types will be given. There are features that are properties of individual

lane marking segments in each triplet (subsection II-C). Furthermore, there are features that are derived from two of the three individual lane marking segments (subsection II-D). Finally, there are features that are derived from all three lane marking segments in a triplet (subsection II-E).

### C. Singleton features

The length  $L$  of each of the three lane marking segments in the triplet is characteristic for lane boundaries. Thus, there are the features  $L_1, L_2, L_3$ .

From the properties  $\Delta g$ ,  $\sigma_i$  and  $\sigma_o$  we form a combined measure of quality  $q = \frac{\Delta g}{\sigma_i + \sigma_o}$ . For each of the three lane marking segments, we evaluate this measure and thus obtain the features  $q_1, q_2, q_3$ .

### D. Double features

Single lane marking segments which belong to the same lane should have the same lengths. We therefore compute the difference of length between two single lane marking segments, normalized to their average length:

$$|\Delta L_{ij}| = \frac{|L_j - L_i|}{\frac{1}{2}(L_j + L_i)}. \quad (1)$$

This gives the features  $|\Delta L_{12}|$  and  $|\Delta L_{23}|$ .

The orientations of successive single lane marking segments should be similar, even for curved lane markings. The difference of orientation is therefore a meaningful quantity and leads to the features  $|\Delta \alpha_{12}|$  and  $|\Delta \alpha_{23}|$ . It is computed as

$$|\Delta \alpha_{ij}| = \begin{cases} |\alpha_i - \alpha_j| & \alpha_i - \alpha_j \in (-\pi/2, \pi/2] \\ |\pi + \alpha_i - \alpha_j| & \alpha_i - \alpha_j \leq -\pi/2 \\ |-\pi + \alpha_i - \alpha_j| & \alpha_i - \alpha_j > \pi/2 \end{cases} \quad (2)$$

The distance between two single lane marking segments normalized to their lengths is another property which gives the features  $|\Delta \mathbf{X}_{12}|$  and  $|\Delta \mathbf{X}_{23}|$ . These are computed as

$$|\Delta \mathbf{X}_{ij}| = \frac{2}{L_i + L_j} \sqrt{(Y_i - Y_j)^2 + (Z_i - Z_j)^2} \quad (3)$$

Lane marking segments which belong to the same lane never overlap, however, segments that are actually clutter sometimes overlap. In order to reflect this, the features  $o_{12}$  and  $o_{23}$  are given by

$$o_{ij} = \frac{\sqrt{(Y_i - Y_j)^2 + (Z_i - Z_j)^2} - \frac{1}{2}L_i - \frac{1}{2}L_j}{\sqrt{(Y_i - Y_j)^2 + (Z_i - Z_j)^2}}. \quad (4)$$

$o_{ij}$  is negative if the lane marking segments overlap, zero if they touch and positive otherwise. The last double feature considers the relation between the lane marking segment orientation and the orientation of a line connecting the lane marking segment to the successive lane marking segment. This orientation difference is denoted by  $|\Delta_{ij}^{\beta\alpha}|$ . The superscript  $\alpha$  refers to the orientation of the lane marking segment and  $\beta$  refers to the orientation of the connecting line.  $|\Delta_{ij}^{\beta\alpha}|$  is small if the segments belong to the same lane. An illustration is given in Fig. 3. This gives the features  $|\Delta_{12}^{\beta\alpha}|$  and  $|\Delta_{23}^{\beta\alpha}|$ .

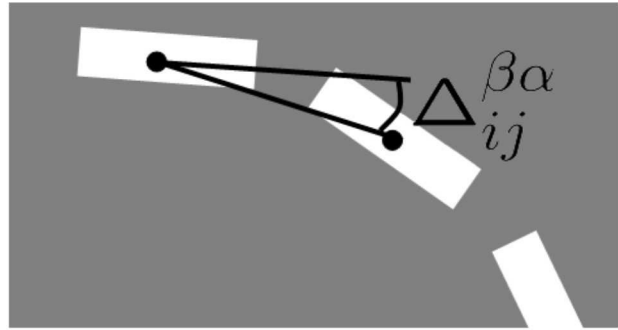


Fig. 3. An illustration of the feature  $|\Delta_{ij}^{\beta\alpha}|$ .

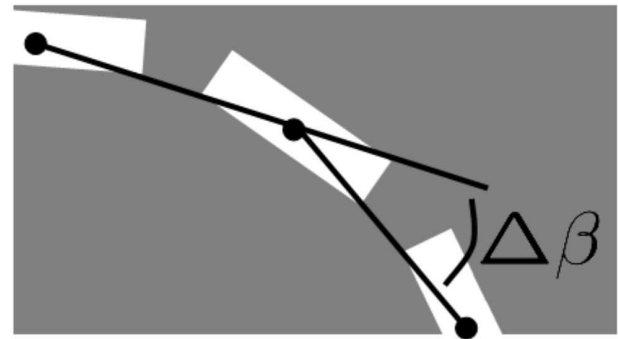


Fig. 4. An illustration of the feature  $|\Delta\beta|$ .

### E. Triplet features

For lanes with constant curvature, the difference of orientation differences is zero. For lanes with a change of curvature, the difference of orientation differences is approximately zero. A significant difference of orientation differences should not occur for a valid lane boundary. The difference of orientation differences is  $|\Delta\Delta\alpha| = |\Delta\alpha_{23} - \Delta\alpha_{12}|$ .

Let a line  $l_{12}$  connect the middle segment and the first segment and let a line  $l_{23}$  connect the middle segment and the third segment in the triplet. Then the difference in orientation  $|\Delta\beta|$  between these two lines is a feature and small if the triplet is part of a lane. An illustration is given in Fig. 4.

Another feature compares the two differences in segment orientation with  $\Delta\beta$ . This is given by

$$|\alpha \min \beta| = \Delta\alpha_{12} + \Delta\alpha_{23} - \Delta\beta. \quad (5)$$

The normalized difference between the two distances  $|\Delta \mathbf{X}_{23}|$  and  $|\Delta \mathbf{X}_{12}|$  is a further feature:

$$\Delta^{nD} |\Delta \mathbf{X}| = \frac{2}{|\Delta \mathbf{X}_{23}| + |\Delta \mathbf{X}_{12}|} (|\Delta \mathbf{X}_{23}| - |\Delta \mathbf{X}_{12}|), \quad (6)$$

The superscript  $nD$  denotes the normalization with respect to the distances. Depending on the type of lane marking, a normalization with respect to the segment lengths rather than the sum of the distances may also be informative which leads to a similar feature

$$\Delta^{nL} |\Delta \mathbf{X}| = \frac{3}{L_1 + L_2 + L_3} (|\Delta \mathbf{X}_{23}| - |\Delta \mathbf{X}_{12}|). \quad (7)$$

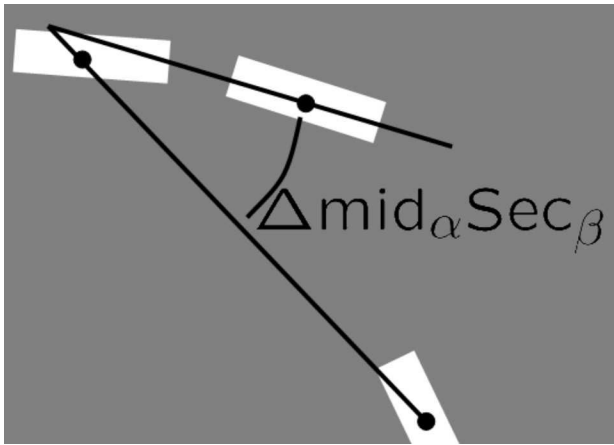


Fig. 5. An illustration of the feature  $|\Delta\text{mid}_\alpha\text{Sec}_\beta|$ .

The final triplet feature is the difference between the orientation of the middle segment and the orientation of the line connecting the first and last segment

$$|\Delta\text{mid}_\alpha\text{Sec}_\beta| = \begin{cases} |\alpha_2 - \beta_{13}| & |\alpha_2 - \beta_{13}| < \pi/2 \\ |\pi + \alpha_2 - \beta_{13}| & \alpha_2 - \beta_{13} \leq -\pi/2 \\ |-\pi + \alpha_2 - \beta_{13}| & \alpha_2 - \beta_{13} > \pi/2 \end{cases} \quad (8)$$

as shown in Fig. 5

Thus, the feature vector consists of 22 elements which are given by  $L_1, L_2, L_3, q_1, q_2, q_3, |\Delta L_{12}|, |\Delta L_{23}|, |\Delta\alpha_{12}|, |\Delta\alpha_{23}|, |\Delta\mathbf{X}_{12}|, |\Delta\mathbf{X}_{23}|, o_{12}, o_{23}, |\Delta_{12}^{\beta\alpha}|, |\Delta_{23}^{\beta\alpha}|, |\Delta\Delta\alpha|, |\Delta\beta|, |\alpha\min\beta|, \Delta^{nD}|\Delta\mathbf{X}|, \Delta^{nL}|\Delta\mathbf{X}|$  and  $|\Delta\text{mid}_\alpha\text{Sec}_\beta|$ . These features describe some of the data that one would expect to be relevant like length, orientation, position and orientation change.

Apart from these features, we evaluated other features like e.g. the segment width. However, these other features have not proven to be meaningful. During preprocessing, we already discard segments with an inappropriate width, thus, the segment width did not vary much throughout the data at the classification stage and therefore provided no additional information. The variation that did exist within the width data was actually mainly due to the quantization error from the image acquisition process and therefore useless for determining lane boundary membership.

The computation of the feature values from the lane marking segment data is computationally inexpensive. For classification, we use a support vector machine [11] with a radial basis function kernel [12]. We scale each feature to the range  $[-1, 1]$ . In order to perform this research, we created an intersection data base consisting of 13 different innercity intersection scenes with corresponding video images and the output of the lane marking segment detector. The overall number of video images is 501 within this data base. On average, the lane marking segment detector found 32.4 lane marking segment hypotheses per image. In the output of the lane marking segment detector, we have labeled 758 lane boundaries consisting of 1642 triplets of single lane

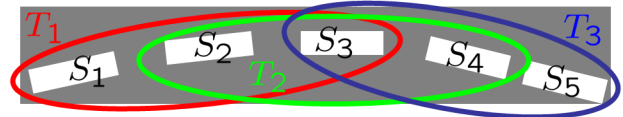


Fig. 6. Combination of three triplets into a sequence of five lane marking segments.

marking segments. We have then split the data base into a training set and a test set for the support vector machine. The intersection scenes in the training set and the test set were not the same. The training set consists of 734 triplets in 206 images and the test set consists of 908 triplets in 295 images. We have trained the support vector machine on the scaled feature space from the training set using grid search and cross validation and have thus determined the parameters  $(C, \gamma)$  for the support vector machine to be  $(C, \gamma) = (8, 0.5)$ . On testing this final support vector machine on the test data, we found that from the 908 labeled correct triplets, 840 were classified as correct and 68 were classified as negative. The test set also contained 1789 triplets labeled as negative, 52 of which were wrongly classified as positive. Overall, our classifier shows a good performance.

The computationally most expensive part about the support vector machine is the training stage. Once the support vector machine has been trained, the application of the support vector machine to the classification is computationally inexpensive.

#### F. Combination to lanes

The detected and as positive classified triplets are combined to form complete lane boundaries. An example is shown in Fig. 6. In case the three triplets  $T_1, T_2, T_3$  have all been found, we obtain the lane boundary consisting of the segments  $S_i, i = 1 \dots 5$ . If one of the triplets has not been classified correctly, the segments will not be combined. We have found that the triplet classification gives such good results that the combination of existing triplets almost always results in valid lane boundaries, without any additional evaluation concerning the combination.

The desired final output is the set of lanes visible on the intersection. Thus, we need to establish which of the lane boundaries are parallel and possibly form a lane. As we do not use a geometrical model, this question cannot be answered by simply comparing parameters of curvature, direction or position. In the following, we give a brief outline of our approach to detect parallel lane boundaries.

Fig. 7 depicts two lane boundaries. We interpolate points between the lane marking segments of each lane boundary, shown in green for the left lane boundary. At each such interpolated point, we take the direction perpendicular to the line connecting the two lane marking segments and form a search area along a distance which corresponds to a typical lane width. At points corresponding to the exact position of lane marking segments, we use the direction perpendicular to the lane marking segment. The search areas are shown as green rectangles. The second lane boundary is also interpola-

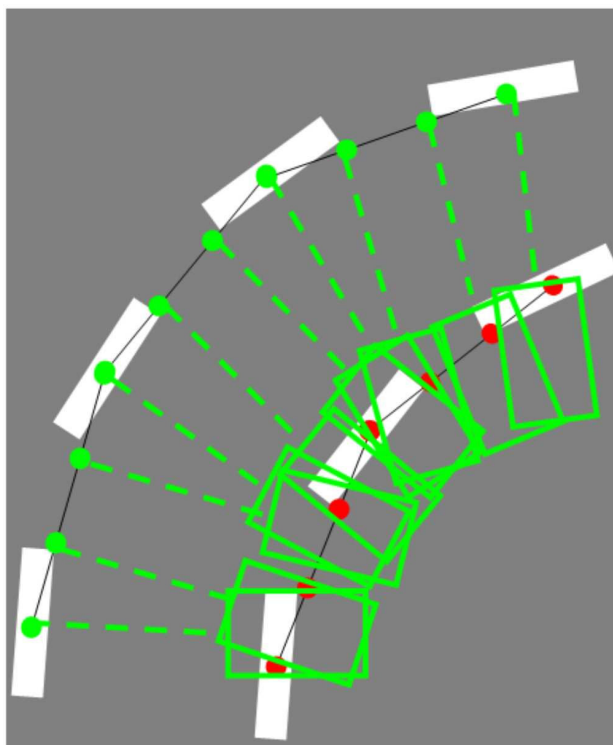


Fig. 7. Test for parallel lanes.

ted, shown in red. It is checked whether a sufficient number of interpolation points from the second lane boundary lies inside the search areas. The test is then applied the other way around. The two lane boundaries are considered to belong to the same lane if a sufficient number of interpolation points of each lane boundary have been found in the search areas coming from the other lane boundary. This approach to test for parallel lane boundaries is applicable to curved lanes independently of any geometrical model. In order to evaluate this detection of parallel lane boundaries, we have manually labeled 96 parallel lane boundaries in our test set. Of these 96 lane boundaries, 90 were determined to be parallel by the test run. The missing six lanes were not discovered because the region of overlap between the boundaries in the direction of the lane was too small. We have not found a single false positive set of parallel lane boundaries in our test set.

### III. RESULTS

We have already described the classification performance of the support vector machine trained and tested with our data base. We have also commented on the performance of the test for parallel lanes. We would now like to give some exemplary detection results based on data obtained from real imagery. The upper portion of Fig. 8 provides a bird's eye view and depicts individual lane marking segments as detected in the grey value image shown in the lower portion. In the bird's eye view, each segment is shown as a white rectangle. Note the segments describing the crossing bicycle lane and the ego lane going to the left. The grey value image contains some snow flakes which result in false positive lane marking

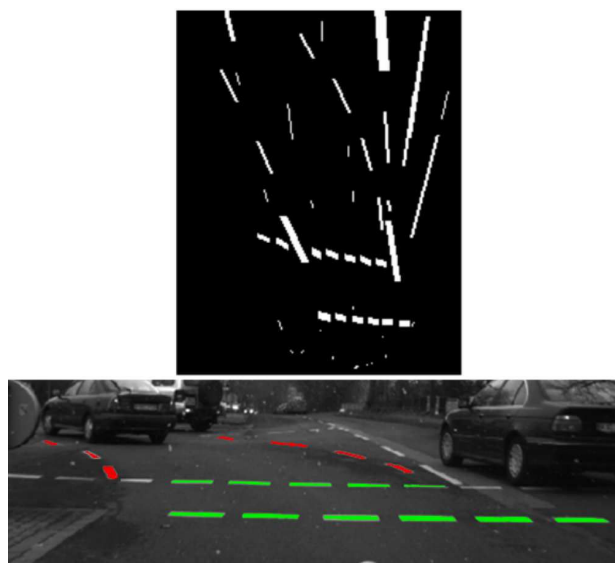


Fig. 8. Detection result. The upper image shows the set of lane marking segments while the lower portion shows the detected lanes.

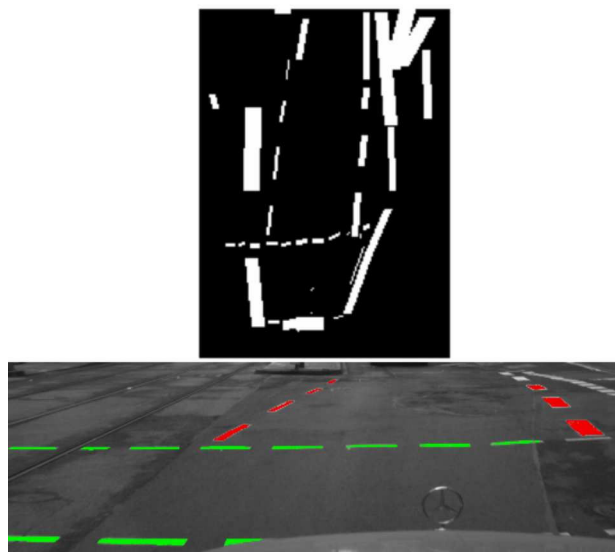


Fig. 9. Detection result. The upper image shows the set of lane marking segments while the lower portion shows the detected lanes.

segments. Our approach successfully detects the crossing bicycle lane and the own lane going to the left. This result is visualized in the lower portion of Fig. 8. Segments that were recognized as belonging to the bicycle lane are painted green and segments that were recognized as belonging to the own lane are painted red.

Fig. 9 shows the lane marking segment data in the upper portion and the corresponding grey value image in the lower portion. The detected pedestrian lane is shown in green and the detected own lane is shown in red.

### IV. CONCLUSION AND OUTLOOK

We have described an approach that detects arbitrarily oriented and curved lanes in a set of lane marking segment

hypotheses. The approach is capable of handling a significant amount of clutter in the data through the formation of lane marking segment triplets. These triplets are classified using a support vector machine. We have successfully tested our approach on data obtained from real imagery depicting complex intersection scenarios.

A possible extension of our research is to integrate the information over time and track the aggregation results.

#### V. ACKNOWLEDGEMENTS

The authors gratefully acknowledge support of this work by the Deutsche Forschungsgemeinschaft (German Research Foundation) within the Transregional Collaborative Research Centre 28 „Cognitive Automobiles“.

#### REFERENCES

- [1] U. Franke. Real time 3d-road modeling for autonomous vehicle guidance. In *7th Scandinavian Conference on Image Analysis*, Aalborg, Denmark, August 1991.
- [2] Ernst D. Dickmanns and Birger D. Mysliwetz. Recursive 3-d road and relative ego-state recognition. *IEEE Transactions on Pattern Analysis and Machine Intelligence*, 14(2):199 – 213, February 1992.
- [3] J. Goldbeck and B. Huertgen. Lane detection and tracking by video sensors. In *IEEE Intelligent Transportation Systems Conf.*, Tokyo, Japan, October 1999.
- [4] Britta Hummel, Zongru Yang, and Christian Duchow. Kreuzungsverstehen – Ein wissenschaftlicher Ansatz. *it – Information Technology, Schwerpunktheft Fahrerassistenzsysteme*, 1, 2007.
- [5] F. Heimes, K. Fleischer, and H.-H. Nagel. Automatic generation of intersection models from digital maps for vision-based driving on innercity intersections. In *IEEE Intelligent Vehicles Symposium*, pages 498 – 503, Dearborn (MI), USA, October 2000.
- [6] K. Kluge and C. Thorpe. The YARF system for vision-based road following. *Mathl. Comput. Modelling*, 22(4-7):213 – 233, 1995.
- [7] W. Enkelmann, G. Struck, and J. Geisler. ROMA - a system for model-based analysis of road markings. In *IEEE Intelligent Vehicles Symposium*, pages 356 – 360, Detroit (MI), USA, September 1995.
- [8] J. Platt. Probabilistic outputs for support vector machines and comparison to regularize likelihood methods. In *Advances in Large Margin Classifiers*, pages 61–74, 2000.
- [9] John Canny. A computational approach to edge detection. *IEEE Transactions on Pattern Analysis and Machine Intelligence*, 8(6):679 – 698, November 1986.
- [10] Christian Duchow. A novel, signal model based approach to lane detection for use in intersection assistance. In *IEEE Intelligent Transportation Systems Conference*, 2006.
- [11] Richard O. Duda, Peter E. Hart, and David G. Stork. *Pattern Classification*. Wiley-Interscience, 2001.
- [12] Chih-Wei Hsu, Chih-Chung Chang, and Chih-Jen Lin. *A Practical Guide to Support Vector Classification*.
- [13] Björn Körtner. Gruppierung von Markierungsdaten innerstädtischer Kreuzungen für die Umfeldsensierung im Automobil. Master's thesis, University of Karlsruhe, 2006.